Multistep Synthesis of Fluorine-Substituted Pyrazolopyrimidine Derivatives With Higher Antibacterial Efficacy Based on *In Vitro* Molecular Docking and Density Functional Theory

Salman A. Khan,[a]* Abdullah M. Asiri,[a,b] R. M. Rahman,[a] Shaaban A. Elroby,[a,c] Faisal M. S. Aqlan,[d] Mohmmad Y. Wani,[e] and Kamlesh Sharma[f]

[a]Chemistry Department, Faculty of Science, King Abdulaziz University, P.O. Box 80203, Jeddah 21589, Saudi Arabia
[b]Center of Excellence for Advanced Materials Research (CEAMR), King Abdulaziz University, P.O. Box 80203, Jeddah 21589, Saudi Arabia
[c]Chemistry Department, Faculty of Science, Benisuief University, Benisuief, Egypt
[d]Chemistry Department, Faculty of Science, Jeddah University, Jeddah, Saudi Arabia
[e]Texas Therapeutics Institute, Brown Foundation Institute of Molecular Medicine, The University of Texas Health Science Center at Houston, 1881 East Road, 77054, Texas, USA
[f]Department of Applied Science, School of Engineering and Technology, ITM University, Sector 23A, Gurgaon 122017, India
*E-mail: sahmad_phd@yahoo.co.in

Received January 13, 2017
DOI 10.1002/jhet.2923
Published online 00 Month 2017 in Wiley Online Library (wileyonlinelibrary.com).

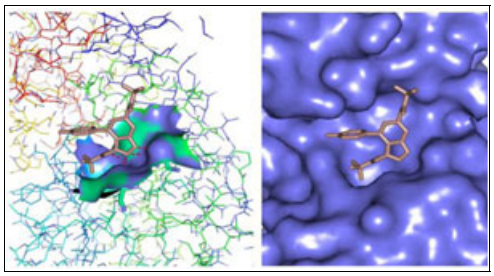

Some new fluorine-substituted pyrazolopyrimidine derivatives (**1.3**–**1.5**) have been synthesized by the multistep reactions, starting from reaction of 4-fluorophenyl malanonitrile (**1**) with guanidine, followed by ring closure reaction with hydrazine to give 2,4-diamino-6-aryl-pyrimidine-5-carbonitrile (**1.2**). Structure of the compounds was conformed by the spectral and elemental analyses. The antibacterial activity of these compounds was tested *in vitro* by the disk diffusion assay against two Gram-positive and two Gram-negative bacteria, and then the minimum inhibitory concentration was determined with reference to the standard drug chloramphenicol. The results showed that compound **1.5** is better at inhibiting growth as compared with chloramphenicol of both types of bacteria (gram-positive and gram-negative). Molecular orbital calculations were carried out by using the density functional theory. The B3LYP/6-311 + G** level of theory was employed to explore LUMO–HOMO gap energy and charge distribution of compounds **1.1** to **1.5**. Docking studies were performed on bacterial glucosamine-6-phosphate synthetase enzyme. Density functional theory calculations and docking studies support the *in vitro* findings.

INTRODUCTION

Gram-positive and Gram-negative pathogens such as *Staphylococcus aureus*, *Staphylococcus pyogenes*, *Salmonella typhimurium*, and *Escherichia coli* are causing food poisoning, rheumatic fever, salmonellosis, diarrhea, and many other infectious diseases [1]. These are serious health problems worldwide. More than 50 million people worldwide are infected, and up to 150 000 die every year due to these bacterial infections [2]. Amoxicillin, norfloxacin, and ciprofloxacin are the principal drugs of choice in the treatment of bacterial infection [3]. But several side effects such as nausea, metallic taste, dizziness, hypertension, and resistance have been reported [4]. After years of misuse and overuse of antibiotics, bacteria are becoming antibiotic resistant, resulting in a potential global health crisis. There is already evidence that antibacterial resistance is associated with an increase in mortality [5]. Frequently, it is recommended to use new antibacterial agents with enhanced broad-spectrum potency. Therefore, recent efforts have been directed toward exploring novel antibacterial agents. Nitrogen-containing heterocyclic compounds with special reference of pyrimidine are prominent, and therefore, various procedures have been worked out for their synthesis [6]. Several pyrimidine derivatives have been found to possess considerable biological activities, which stimulated research activity in this field. Their prominent effects are, for example, antimicrobial [7], central nervous system [8], and immunosuppressive [9] activities. There are several substituted pyrazolines that have bleaching property or

© 2017 Wiley Periodicals, Inc.

act as luminescent and fluorescent agents [10]. They are also useful as biodegradable agrochemicals [11]. Bicyclic pyrazolopyrimidine derivatives dramatically increase the biological activates such as antibacterial [12], analgesic [13], anti-inflammatory [14], antiviral [15,16], antifungal [17], antiarthritic [18], cerebroprotective effect [19], and antidepressant [20]. In addition, introduction of fluorine atoms to heterocyclic nitrogen systems enhances and improves their pharmacological properties such as enhancing the electrostatic force and hydrophobic binding stability against metabolic transformations [21–23].

Encouraged by these facts and in continuation with the work related to the synthesis, spectral studies, and biological properties of pyrazolopyrimidine, the synthesis of some novel pyrazolopyrimidine is reported here. Furthermore, the geometric structures of synthesized compounds were also computationally calculated by using density functional theory with RB3LYP method and interaction of the compounds with their probable target was established by docking studies.

RESULTS AND DISCUSSION

Chemistry. In the present work, pyrazolopyrimidine derivatives (**1.3**, **1.4**, and **1.5**) were prepared by the multistep reaction [24]. The synthetic route of compounds is outlined in Scheme 1. The chemical structures of the synthesized compounds were established by spectroscopic (FT-IR, ^{1}H-NMR, ^{13}C-NMR, and mass) and elemental analysis. Based on these facts, the present work reports an easy and efficient route for the synthesis of fluorine-substituted pyrazolopyrimidines in view of their antibacterial effects. Thus, cycloaddition of arylidene malononitrile **1.1** with guanidine hydrochloride in refluxing absolute ethanol-anhydrous K_2CO_3 yielded the 2,4-diamino-6-(4-fluorophenyl)pyrimidin-5-carbonitrile **1.2**. The structure of **1.2** was deduced from that spectral data. IR spectrum showed the absorption bands at ν 3289, 2225, and 1250 cm^{-1} for NH, CN, and C─F function groups, while ^{1}H-NMR spectrum recorded resonated signals at δ 9.97 and 9.73 ppm attributed to two NH_2

Scheme 1. Synthesis of fluorine-substituted pyrazolopyrimidine derivatives. [Color figure can be viewed at wileyonlinelibrary.com]

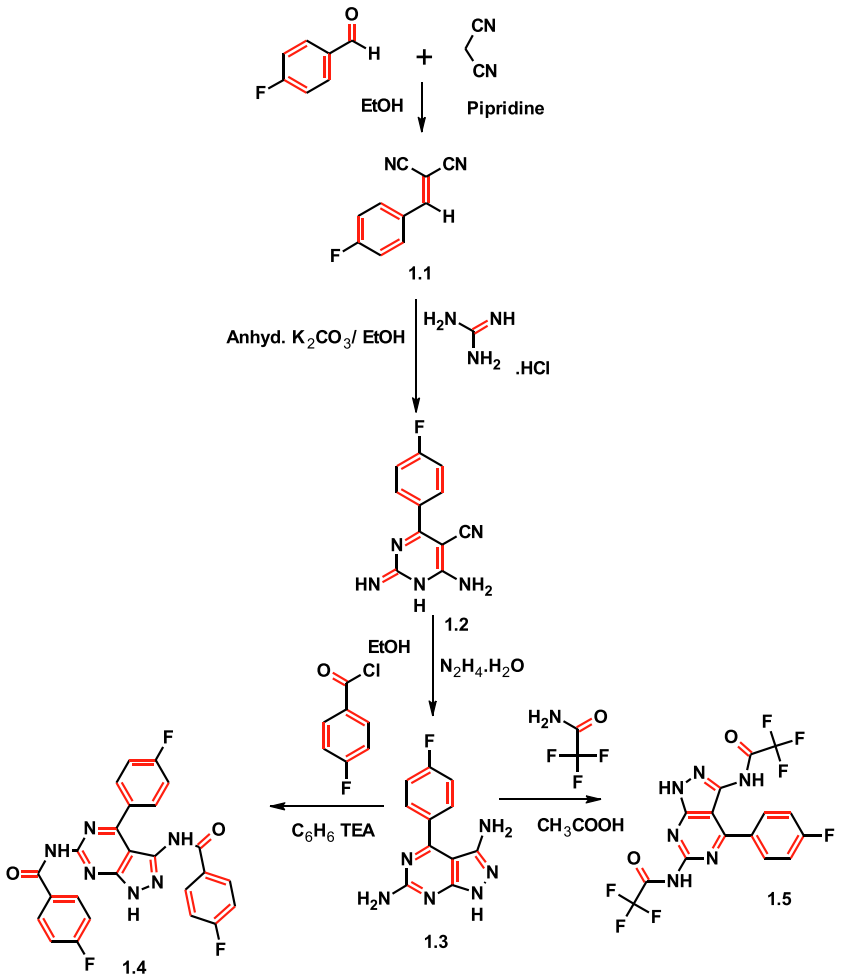

protons. Also, ^{13}C-NMR exhibited resonated signals at δ 168.91, 50.74, and 24.35 ppm for NH═C, C─F, and C─N. It is interesting that a simple nucleophilic attack of hydrazine hydrate to a more electrophilic carbon of CN in refluxing absolute ethanol afforded 4-(4-fluorophenyl)-1*H*-pyrazolo[3,4-D]pyrimidine-3,6-diamine (**1.3**) via loss 1 mol of NH_3.

The former structure of **1.3** was established from the ^{1}H-NMR, which showed δ at 8.62, 8.61, and 8.56 ppm due to the presence of NH_2, NH_2, and NH. Also, IR spectrum showed the lacks of CN group. The full fluorinated pyrazolo[3,4-*b*]pyrimidine derivatives **1.4** and **1.5** have been obtained from fluorinated acylation and/or benzeylation of compound **1.3** via warming with trifluoroacetamide and/or 4-fluorobeneyl chloride in acetic acid or dry C_6H_6-TEA (Scheme 1).

The fine structure of compounds **1.4** and **1.5** was deduced from corrected elemental analysis and their spectral data. ^{1}H-NMR of **1.4** showed resonated signals at δ 7.82 and 7.53 ppm for the NH, while ^{13}C-NMR recorded resonated signals at δ 176.40 and 169.24 ppm for two C═O carbons, in addition at δ 25.47, 25.42, and 24.35 ppm for their C─F. The IR spectrum of **1.4** exhibited the absorption bands at ν 1637 cm^{-1} and attributed ─CONH-functional groups.

Finally, the former structure of **1.5** was supported from its ^{13}C-NMR, which showed δ at 170.73 and 167.14 ppm for two CO–CF_3 and 165.45 ppm for CF_3. ^{1}H-NMR spectrum exhibited resonated signals at δ 8.14, 8.11, and 7.89 ppm for three NH groups. In addition, mass fragmentation measurement recorded the M^+ +1 at 438 by 56% with a base peak at 95 with 100%.

In vitro screening: disc-diffusion and microdilution assay. The compounds (**1.1**–**1.5**) were tested for their antibacterial activities by disk-diffusion method by using nutrient broth medium [contained (g/L): beef extract 3 g; peptone 5 g; pH 7.0] [25,26]. The Gram-positive bacteria and Gram-negative bacteria utilized in this study consisted of *S. aureus*, *S. pyogenes*, *S. typhimurium*, and *E. coli*. In the disk-diffusion method, sterile paper discs (0.5 mm) impregnated with compound dissolved in dimethyl sulfoxide (DMSO) at concentration of 100 μg/mL were used. Then, the paper discs impregnated with the solution of the compound tested were placed on the surface of the media inoculated with the microorganism. The plates were incubated at 35°C for 24 h. After incubation, the growth inhibition zones are shown in Table 1. The compounds were further checked by MIC method. The results are presented in Table 2.

Molecular orbital calculations. B3LYP/6-311 + G** level of theory was employed to investigate the electronic c structure of the compounds **1.1** to **1.5**. Highest occupied molecular orbitals (HOMOs), lowest unoccupied molecular orbitals (LUMOs), and Frontier molecular orbitals (FMOs) can be used to characterize the chemical reactions. The HOMO energy characterizes the ability to donate an electron, and LUMO energy characterizes the ability to obtain an electron. The energy gap (LUMO–HOMO) is also used for determining the molecular chemical stability and biological activity.

The energies of the FMOs of the five studied compounds, HOMO, LUMO, and energy gap were calculated at B3LYP/6-311 + G(d,p) theory level to explore the relation between the activity and electronic structure. HOMO, LUMO, energy gap, and the optimized geometric structure of the studied compounds (**1.1**–**1.5**) are presented in Table 3 and Figure 1, which display the electron densities of the FMOs (HOMO and LUMO) for the five molecules.

As can be seen from Figure 1, The LUMO is mainly delocalized among all the atoms for all molecules, except compounds **1.4** and **1.5**. On other hand, the HOMOs are localized on the nitrogen atoms, except in compounds **1.1** and **1.5**. The FMOs for compound **1.5** have unique electron density distribution properties than other compounds. Besides these distributions, the LUMO energy value (2.96 eV) for compound **1.5** is high. The mean value of the energy gap for the studied compounds

Table 1

Antibacterial activity of synthesized compounds (1.1–1.5), positive control chloramphenicol (chlora.), and negative control (DMSO) measured by the Halo Zone Test (unit, mm) and their cytotoxicity.

Compounds	Corresponding effect on microorganisms				Cytotoxicity activity IC_{50} (in m*M*/mL) (L123 cell)
	S. aureus	*S. pyogenes*	*S. typhimurium*	*E. coli*	
1.1	8.8 ± 0.3	8.6 ± 0.2	9.0 ± 0.3	8.2 ± 0.4	
1.2	11.2 ± 0.2	9.2 ± 0.4	10.2 ± 0.3	10.6 ± 0.2	
1.3	14.2 ± 0.3	15.4 ± 0.4	14.8 ± 0.4	13.4 ± 0.4	50
1.4	16.2 ± 0.3	17.4 ± 0.5	16.2 ± 0.4	18. 2 ± 0.1	>100
1.5	19.6 ± 0.2	18.8 ± 0.3	16.8 ± 0.4	22.4 ± 0.4	50
Chlora.	17.0 ± 0.5	18.2 ± 0.4	17.2 ± 0.8	20.0 ± 0.2	
DMSO					

Table 2

Minimum inhibition concentration (MIC) of synthesized compounds (**1.1**–**1.5**) products, positive control: chloramphenicol.

	MIC (μg mL^{-1}) compound					Positive
Bacterial strain	**1.1**	**1.2**	**1.3**	**1.4**	**1.5**	control
S. aureus	512	512	128	64	16	32
S. pyogenes	512	256	64	32	16	32
S. typhimurium	512	512	256	64	32	32
E. coli	512	256	128	64	32	32

is found around 4.25 eV. This value makes these compounds chemically quite stable and reactive as antibacterial, especially compound 1.5. In conclusion, compound **1.5** has low gap energy and high LUMO energy value, which makes this structure as a good antibacterial. These results are in good agreement with the experimental results.

Molecular docking. Docking of the target compound **1.5** into GlmS active site revealed that several molecular interactions were responsible for the observed affinity. The best docking energy model and most possible interaction mode between ligand (**1.5**) and GlmS are shown in Figure 2. It was observed that the compound mainly interacts with glucosamine-6-phosphate synthase by binding at active sites SER-303, SER-349, GLN-349, and THR-352. The binding affinity values of the docked target compound (**1.5**) were found to be −7.3 kcal mol^{-1}. The results reveal that the nitrogen atoms of the pyrazole ring show strong hydrogen bonding interaction with the amino acid residues of the protein, which clearly advocates its better antibacterial efficacy. From these results, it can be inferred that the compounds probably show their antibacterial activity by inhibiting the glucosamine-6-phosphate synthetase enzyme, which is an important enzyme for bacterial cell wall formation. Therefore, these preliminary results indicate that pyrazole derivatives can be the most promising therapeutic agents against bacterial infections, which needs further optimization. The strategy presented here therefore has potential for the discovery of novel GlmS inhibitors as antibacterial agents.

Cytotoxicity against L123 (human lung cells). Cytotoxicity was performed by MTT assay method [27]. A 96-well flat bottom tissue culture plate was seeded with 2×10^3 cells in 0.1 mL of MEM medium supplemented with 10% FBS and allowed to attach for 24 h. After 24 h of incubation, the cells were treated with test compounds to obtain concentrations of 5, 10, 20, 50, and 100 m*M*/mL incubated for 48 h. The cells in the control group received only the medium containing the 0.2% DMSO. Each treatment was performed in duplication. After the treatment, drug-containing media were removed and washed with 200 mL of phosphate-buffered saline. To each well of the 96-well plate, 100 mL of MTT reagent (stock: 1 mg/mL in serum-free medium) was added and incubated for 4 h at 37°C. After 4 h of incubation, the plate was inverted on tissue paper to remove the MTT reagent. To solubilize formazan crystals in the wells, 100 mL of 100% DMSO was added to each well. The optical density was measured by microtiter plate reader at 590 nm. Compound concentration (m*M*) is required to reduce the viability of mock-infected cells by 50% as determined by MTT method, which is summarized in Table 1. The results of MTT assay are mentioned on the cell viability based on the ability to metabolize the compounds. The results show that compound **1.4** is comparatively more cytotoxic than **1.3** and **1.5**, as these derivatives showed IC_{50} values more than 100 m*M*/mL. It means that 4-(4-fluorophenyl)-1*H*-pyrazolo [3,4-D]pyrimidine-3,6-diamine (1.3) and 3,6-di (trifluoroacetamide)-4-(4-fluorophenyl)-1*H*-pyrazolo[3,4-D]pyrimidine (1.5) derivative showed higher cytotoxicity that is dose-related.

EXPERIMENTAL

All chemicals and solvents used for this work were obtained from Merck (Germany) and Aldrich chemical company (USA). The melting points of the synthesized compounds were determined in open-glass capillaries on Stuart-SMP10 melting point apparatus (Staffordshire, UK) and are uncorrected. IR absorption spectra were recorded on Shimadzu FTIR-8400s (Kyoto, Japan) by using KBr pellets in the range of 4000–400 cm^{-1}. ^{1}H-NMR and ^{13}C-NMR spectra were recorded on BRUCKER-AVANCE-III 600-MHz spectrophotometer (Karlsruhe, Germany) and TMS (tetramethylsilane) as an internal standard. The ^{1}H-NMR and ^{13}C-NMR chemical shifts were reported as parts per million (ppm) downfield from TMS (Me_4Si). The splitting patterns are designated as follows: s, singlet; d, doublet; m, multiplet. Mass spectra were recorded on EI-MS spectrometer. IR, ^{1}H-NMR, ^{13}C-NMR, and mass spectra were consistent with the assigned structures. Elemental analyses (C, H, and N) were done on a CHN rapid analyzer. All the new compounds gave C, H, and N analyses within 0.03% of the theoretical values. Purity of the compounds was checked by thin-layer chromatography (TLC) on Merck silica gel $60F_{254}$ precoated sheets in chloroform/methanol mixture, and spots were developed by using iodine vapors/ultraviolet light as visualizing agent.

4-Fluorobenzylidene-propanedinitrile (1.1). A mixture of 4-fluorobenzylaldehyde 3 g (0.024 mol) and malononitrile 1.59 g (0.024 mol) in anhydrous ethanol (15 ml), in the presence of a few drops of pyridine, was refluxed at 80°C for 3 h with continuous stirring. The progress of the reaction was monitored by TLC. After completion of the reaction, the solution was cooled. The heavy precipitate thus obtained was collected by filtration

Table 3

Optimized geometric structures and FMO energies of compounds **1.1** to **1.5** calculated by using DFT/RB3LYP/6-311 + G** level of theory.

Structures	HOMO	LUMO	Energy gap
		eV	
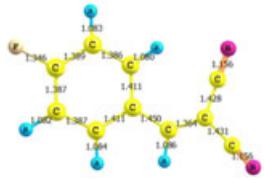	−7.452	−3.345	4.107
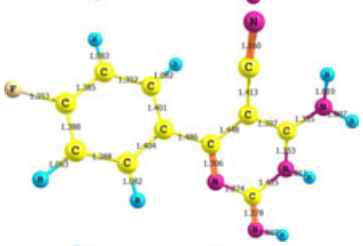	−6.429	−2.130	4.298
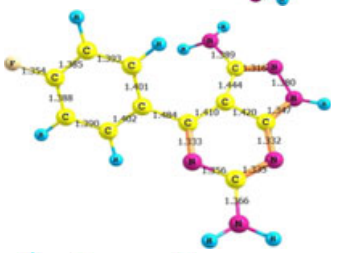	−5.965	−1.857	4.108
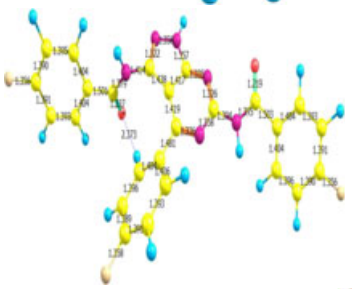	−6.813	−2.319	4.494
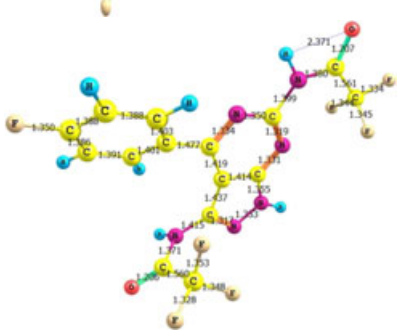	−7.385	−2.964	4.421

and purified by recrystallization from a mixture of methanol and chloroform.

Dark orange solid (chloroform); yield: 78%; mp 112°C; ^{1}H-NMR (DMSO-d_6) (δ/ppm): 7.92 (s, CH═C), 7.80 (d, CH aromatic, J = 7.6 Hz), 7.78 (d, CH aromatic, J = 7.8 Hz), 6.96 (d, CH aromatic, J = 7.8 Hz), 6.82 (d, CH aromatic, J = 7.6 Hz); ^{13}C-NMR (DMSO-d_6) (δ/ppm): 166.9, 165.2, 158.2, 154.4, 133.9, 127.3, 119.7, 114.7, 25.3, 24.3; EI-MS *m/z* (rel. int.%): 173 (56) $[M + 1]^+$; IR (KBr) ν_{max} cm^{-1}: 3256 (Ar─H), 2951 (C─H), 1597 (C═C), 1508 (HC═N). *Anal*. Calcd. for $C_{10}H_5N_2$: C, 69.77, H, 2.93, N, 16.27. Found: C, 69.74, H, 2.89, N, 16.23.

6-Amino-4-(4-fluorophenyl)-2-imino-1,2-dihydropyrimidine-5-carbonitrile (1.2). A mixture of 4-fluorobenzylidene-propanedinitrile (**1**) 2 g (0.0116 mol) guanidine hydrochloride (0.0120 mol) in anhydrous ethanol (15 mL),

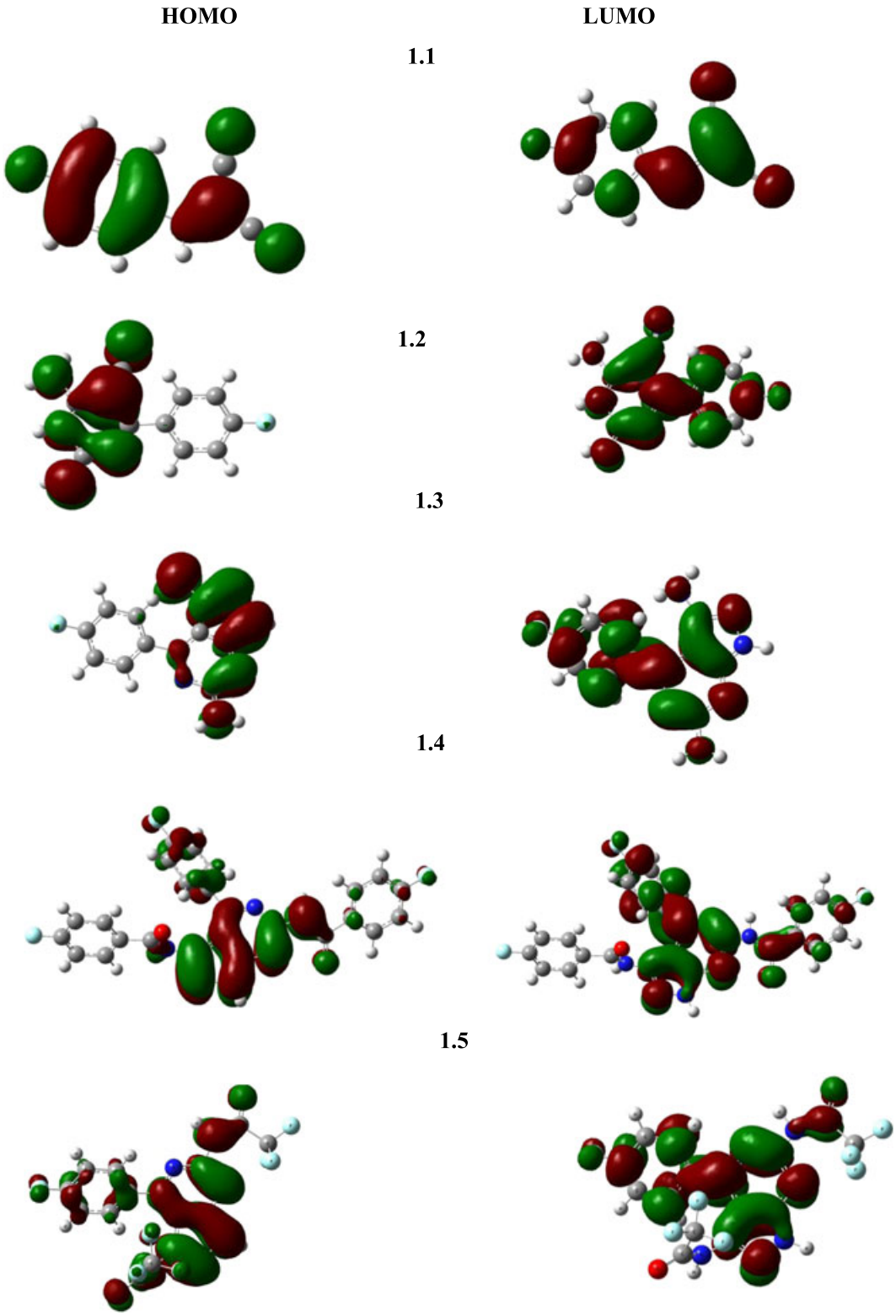

Figure 1. The electronic densities of HOMO and LUMO for compounds **1**–**5** using B3LYP/6-311 + G** level of theory. [Color figure can be viewed at wileyonlinelibrary.com]

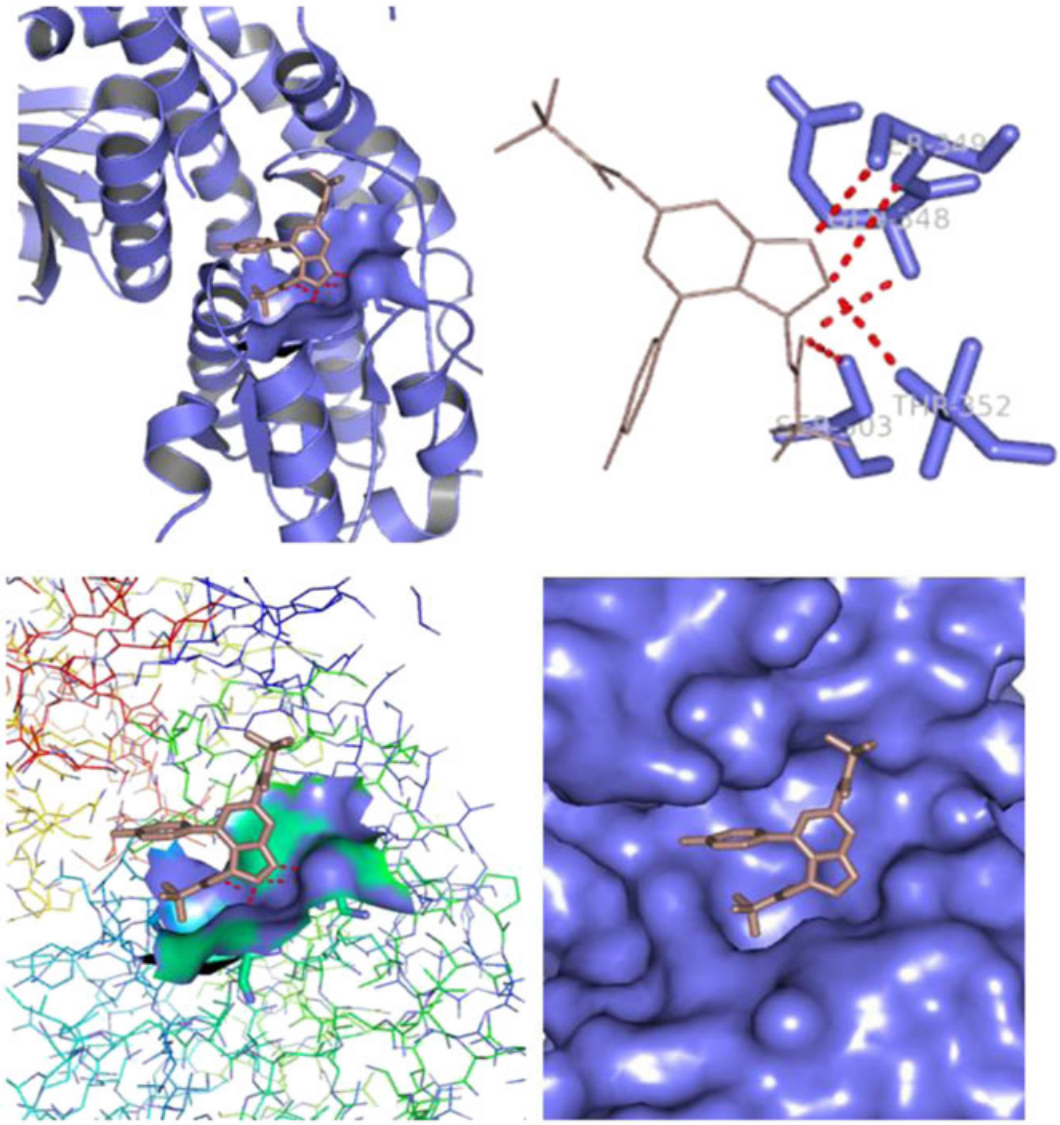

Figure 2. Compound (**1.5**) showing interaction with SER-303, SER-349, GLN-349, and THR-352 residues of the bacterial G-6-P synthetase protein (different poses of the ligand protein interaction are shown in cartoon and surface view). Compound is represented by sticks in gray color. Hydrogen bonds represented by using dashed lines (red). Images are visualized by using PYMOL. [Color figure can be viewed at wileyonlinelibrary.com]

in the presence of K_2CO_3, was refluxed at 80°C for 6 h with continuous stirring. The progress of the reaction was monitored by TLC. After completion of the reaction, the solution was cooled. The heavy precipitate thus obtained was collected by filtration and purified by recrystallization from a mixture of methanol and chloroform.

Dark orange solid (chloroform); yield: 72%; mp 128°C; ^{1}H-NMR (DMSO-d_6) (δ/ppm): 9.97 (s, NH_2), 9.73 (s, NH_2), 7.32–7.02 (m, 4H, CH aromatic); ^{13}C-NMR (DMSO-d_6) (δ/ppm): 168.9, 165.3, 162.6, 159.5, 151.2, 132.4, 131.9, 130.7, 129.0, 116.9, 50.7, 24.3; EI-MS *m*/*z* (rel. int.%): 231(62) $[M + 1]^+$; IR (KBr) ν_{max} cm^{-1}: 3289 (N─H), 2923 (C─H), 2225 (CN), 1571 (C═C), 1507 (C═N), 1250 (C─F), 1155 (C─N). *Anal*. Calcd. for $C_{11}H_8FN_5$: C, 57.64, H, 3.52, N, 30.55. Found: C, 57.61, H, 3.45, N, 30.48.

4-(4-Fluorophenyl)-1H-pyrazolo[3,4-d]pyrimidine-3,6-diamine (1.3). A mixture of 6-amino-4-(4-fluorophenyl)-2-imino-1,2-dihydropyrimidine-5-carbonitrile (**2**) 1.5 g (0.0065 mol) was refluxed with hydrazine hydrate (0.0070 mol) in dry EtOH (30 mL) and was heated at 80° C for 4 h. The progress of the reaction was monitored by TLC. After completion of the reaction, the solvent was removed under reduced pressure and the residue obtained was purified by column chromatography (20:80, diethyl ether: petroleum ether). The obtained solid was crystallized from EtOH to yield compound no. 3. dark brown solid.

Dark orange solid (chloroform); yield: 65%; mp 154°C; ^{1}H-NMR (DMSO-d_6) (δ/ppm): 8.62 (s, NH_2), 8.61 (s, NH_2), 8.56 (s, NH), 7.38–6.90 (m, 4H, CH aromatic); ^{13}C-NMR (DMSO-d_6) (δ/ppm): 168.9, 165.3, 160.9, 141.9, 132.4, 130.6, 127.8, 114.3, 50.7, 25.8, 15.1; EI-MS *m*/*z* (rel. int.%): 246 (65) $[M + 1]^+$; IR (KBr) ν_{max} cm^{-1}: 3388 (NH_2), 3251 (N─H), 3221 (Ar─H), 2951 (C─H), 1558 (C═N), 1153 (C─N). *Anal*. Calcd. for $C_{11}H_9FN_6$: C, 54.10, H, 3.71, N, 34.41. Found: C, 54.07, H, 3.67, N, 34.33.

3,6-Di(4-fluorobenzamide)-4-(4-fluorophenyl)-1H-pyrazolo[3,4-d]pyrimidine (1.4). A mixture of 4-(4-fluorophenyl)-1*H*-pyrazolo[3,4-D]pyrimidine-3,6-diamine (**1.3**) (**3**) (0.3 g, 0.0012 mol) and 4-fluorobenzoyl chloride (0.0028 mol) in 15 mL of DMF in the presence of a few drops of TEA was refluxed at 80°C for 8 h with continuous stirring. The progress of the reaction was monitored by TLC. After the completion of the reaction, the reaction mixture was poured into ice water to obtained precipitated solid and was filtered and recrystallized in methanol.

Dark orange solid (chloroform); yield: 75%; semisolid ^{1}H-NMR (DMSO-d_6) (δ/ppm): 7.82 (s, NH), 7.53 (s, NH), 7.28–6.20 (m, 12H, CH aromatic); ^{13}C-NMR (DMSO-d_6) (δ/ppm): 176.4, 169.2, 165.0, 163.6, 162.2, 131.8, 131.8, 130.6, 130.6, 129.9, 128.9, 116.8, 116.2, 116.1, 115.9, 115.7, 114.2, 78.6, 48.9, 44.6, 25.5, 25.4, 24.3, 22.6. EI-MS *m*/*z* (rel. int.%): 490 (76) $[M + 1]^+$; IR (KBr) ν_{max} cm^{-1}: 3262 (N─H), 2951(C─H), 1637 (C═O), 1597 (C═C), 1529 (C═N), 1150 (C─N). *Anal*. Calcd. for $C_{25}H_{15}F_3N_6O_2$: C, 61.48, H, 3.10, N, 17.21. Found: C, 61.38, H, 3.07, N, 17.16.

3,6-Di(trifluoroacetamide)-4-(4-fluorophenyl)-1H-pyrazolo[3,4-d]pyrimidine (1.5). A mixture of 4-(4-fluorophenyl)-1*H*-pyrazolo [3,4-D]pyrimidine-3,6-diamine (**1.3**) (**3**) (0.3 g, 0.0012 mol) and trifluoroacetyl chloride (0.0028 mol) in 15 mL of acetic acid was refluxed at 80°C for 8 h with continuous stirring. The progress of the reaction was monitored by TLC. After the completion of the reaction, the reaction mixture was poured into ice water. The obtained precipitated solid was filtered and recrystallized in methanol. Dark orange solid (chloroform); yield: 78%; mp 166°C; ^{1}H-NMR (DMSO-d_6) (δ/ppm): 8.14 (s, NH), 8.11 (s, NH), 7.89 (s, NH), 7.42–7.02 (m, 4H, CH aromatic); ^{13}C-NMR (DMSO-d_6) (δ/ppm): 170.7, 167.1, 165.4, 132.8, 132.8, 125.6, 125.6, 115.8, 115.7, 115.7, 115.6, 125.5, 115.3, 45.9, 8.6. EI-MS *m*/*z* (rel. int.%): 438 (56) $[M + 1]^+$; IR (KBr) ν_{max} cm^{-1}: 3319 (N─H), 2948 (C─H), 1672 (C═O), 1558 (C═C), 1524 (C═N), 1128 (C─N). *Anal*. Calcd. for $C_{15}H_7F_7N_6O_2$: C, 41.30, H, 1.62, N, 19.26. Found: C, 41.25, H, 1.56, N, 19.19.

Organism culture and in vitro screening. Antibacterial activity was assayed by the disk-diffusion method with minor modifications. *S. aureus*, *S. pyogenes*, *S. typhimurium*, and *E. coli* were subcultured in Brain Heart Infusion medium and incubated for 18 h at 37°C, and then the bacterial cells were suspended according to the McFarland protocol in saline solution to produce a suspension of about 10^5 cfu mL^{-1}. Ten microliters of this suspension was mixed with sterile antibiotic agar (10 mL) at 40°C and poured onto an agar plate in a laminar flow cabinet. Five paper disks (6.0 mm diameter) were fixed onto a nutrient agar plate. Ten milligrams of each test compound was dissolved in DMSO (100 μL) to prepare stock solution, and from the stock solution, different concentrations of 10 (1 μL of stock solution + 9 μL of solvent), 20 (1 μL of stock solution + 4 μL of solvent), 25 (1 μL of stock solution + 3 μL of solvent), 50 (1 μL of stock solution + 1 μL of solvent), and 100 μg/μL of each test compound were prepared. These compounds of different concentrations were poured over a disk plate. Chloramphenicol (30 μg) was used as standard drug (positive control). A DMSO-wetted disk was used as negative control. The susceptibility of the bacteria to the test compounds was determined by the formation of an inhibitory zone after 18 h of incubation at 36°C. Table 1 reports the inhibition zones (mm) of each compound, and the controls in this experiment were repeated two times for each compound and found the same results.

Theoretical method. The computational calculation of compounds **1.1**–**1.5** was performed by using SPARTAN'08 Windows graphical software with density functional theory, DFT/6-31G* basis set [28]. This method has been previously used successfully for the small molecule's calculations [29]. The fundamental frequencies of optimized structure were also calculated and assigned as minima (no negative frequencies).

Docking studies. The 3D structures of the target compound (**1.5**) were created by CHEM DRAW ULTRA 8.0 and converted to the pdb file format. Ligand preparation was conducted by assigning Gastegier charges, merging nonpolar hydrogens, and saving it in pdbqt file format by using AUTODOCK TOOLS 4.2. The crystal structure of the glucosamine-6-phasphate synthase was downloaded from Protein Data Bank (http: //www.rcsb.org/pdb. Code: 2VF4). AUTODOCK used the local search to search for the optimum binding site of small molecules to the protein. The active site was defined by a grid box of 80 × 60 × 88 points and spacing of 0.375 Å with the ligand binding site as the center. The final structure was then saved in pdbqt format. Molecular docking calculations were carried out with AUTODOCK VINA [30]. The conformation with the lowest binding free energy was used for analysis. All molecular docked models were prepared by using PYMOL viewer.

CONCLUSION

Based on the DFT/RB3LYP model, some heterocyclic compounds were synthesized and screened for the

antibacterial activity. Some new fluorine substituted pyrazolo[4, 5-e]pyrimidine derivatives (**1.3**–**1.5**) were synthesized starting from the reaction of 4-fluorophenyl malanonitrile **1.1** with guanidine, followed by ring closure reaction with hydrazine to give 2,4-diamino-6-aryl-pyrimidine-5-carbonitrile (**1.2**). The antibacterial activity of these compounds was examined and the results showed that **1.4** and **1.5** display increased antibacterial activity compared to the reference drug. Among all the five compounds, triflurobispyrazolopyrimidine (**1.5**) derivative showed better antibacterial activity on both types of bacteria than the reference drug chloramphenicol. It was observed theoretically that the compound with lower LUMO value and higher density value has shown the highest activity. Our theoretical results were found in good corroboration with the experimental results. Structure activity relationship studies revealed that fluorine-substituted derivatives play an important role in antimicrobial activity. A little structure variation can cause immense difference in the activity of the drug. This approach can open new vistas in the chemotherapy of the infective disease. The field is further open for pharmacokinetics and clinic studies to establish these molecules as drugs in the market.

Acknowledgments. The authors are thankful to the Chemistry Department at King Abdulaziz University for providing research facilities.

REFERENCES AND NOTES

[1] Thomson, G. T. D.; DeRubeis, D. A.; Hodge, M. A.; Rajanayagam, C.; Inman, R. D. J Med 1995, 98, 13.

[2] Asiri, A. M.; Khan, S. A. J Heterocycl Chem 2012, 49, 1452.

[3] Naber, K. G.; Wullt, B.; Wagenlehner, F. M. E. Int J Antimicrob Ag 2011, 38, 21.

[4] Khan, S. A.; Asiri, A. M. Chin J Chem 2012, 30, 1901.

[5] Tonk, R. K.; Bawa, S.; Chawla, G.; Deora, G. S.; Kumar, S.; Rathore, V.; Mulakayala, N.; Rajaram, A.; Kalle, A. M.; Afzal, O. Eur J Med Chem 2012, 57, 176.

[6] Asir, A. M.; Khan, S. A. Molecules 2010, 15, 6850.

[7] Asiri, A. M.; Khan, S. A. J Heterocycl Chem 2012, 49, 1434.

[8] Mukaiyama, H.; Nishimura, T.; Kobayashi, S.; Komatsu, Y.; Kikuchi, S.; Ozawa, T.; Kamada, N.; Ohnota, H. Bioorg Med Chem 2008, 16, 909.

[9] Xu, X.; Williams, J. W.; Gong, H.; Finnegan, A.; Chong, A. S. F. Biochem Pharmacol 1996, 52, 527.

[10] Wilkinson, F.; Kelly, G. P.; Michael, C.; Oelkrug, D. J Photochem PhotobiolB 1990, 52, 309.

[11] Chandanshive, J. Z.; Gonzalez, P. B.; Tiznado, W.; Bonini, B. F.; Caballero, J.; Femoni, C.; Franchini, M. C. Tetrahedron 2012, 68, 3319.

[12] Suresh, L.; Kumar, P. S. V.; Poornachandra, Y.; Kumar, C. G.; Chandramouli, G. V. P. Bioorg Med Chem Lett 2017, 15, 1451.

[13] Chobe, S. S.; Dawane, B. S.; Tumbi, K. M.; Nandekar, P. P.; Sangamwar, A. T. Bioorg Med Chem Lett 2012, 22, 7566.

[14] Shaaban, M. S.; Saleh, T. S.; Mayhoub, A. S.; Mansour, A.; Farag, A. M. Bioorg Med Chem 2008, 176, 6344.

[15] Moukha-chafiq, O.; Taha, M. L.; Lazrek, H. B.; Vasseur, J. J.; Pannecouque, C.; Witvrouw, M.; De Clercq, E. Il Farmaco, 2002, 57, 27.

[16] Braun, H.; Riabova, B.; Komarova, E. S.; Richter, M. P.; Wutzler, M. P.; Schmidtke, M. Antiviral Res 2011, 90, A29.

[17] Novinson, T.; Robins, R. K.; Matthews, T. R. J. Med Chem 2010, 20, 296.

[18] Revesz, L.; Blum, E.; Di Padova, F. E.; Buhl, T.; Feifel, R.; Gram, H.; Hiestand, P.; Manning, U.; Neumann, U.; Rucklin, G. Bioorg Med Chem Lett 2006, 16, 262.

[19] White, T. D.Eur J Pharmacol 1996, 303, 27.

[20] Abdel-Gawad, S. M.; El-Gaby, M. S. A.; Ghorab, M. M. Il Farmaco 2000, 55, 287.

[21] Ismail, F. M. D. J. Fluorine Chem 2002, 118, 27.

[22] Reddy, M. D.; Fronczek, F. R.; Blake Watkins, E. B Org Lett 2016, 18, 5620.

[23] Ojima, I.; Carthy, J. R.; Welch, J. T. Biomdical Frontiers of fluorine Chemistry; ACS Symposium Series 639; American Chemical Society: Washington, DC, 1996.

[24] Fikry, R. M. Ind J Hetrocycl Chem 1995, 4, 265.

[25] Asiri, A. M.; Khan, S. A. Molecules 2011, 16, 523.

[26] Khan, S. A.; Asiri, A. M.; Alamry, K. A.; El-Daly, S. A.; Zayed, M. A. M. Russi J Bioorg Chem 2013, 39, 353.

[27] Heilmann, J.; Wasescha, M. R.; Schmidt, T. J. Bioorg Med Chem 2001, 9, 2189.

[28] Spartan'08 version 1.2.0, Wavefunction, Inc., 18401 Von Karman Ave., Suite 370, Irvine, CA 92612, USA. https://www.wavefun.com/support/sp_win/support_winLV.html

[29] Asiri, A. M.; Khan, S. A.; Marwani, H. M.; Sharma, K. J. Phtochem Phtobio B 2013, 120, 82.

[30] Trott, O.; Olson, A. J. J Comput Chem 2010, 31, 455.